Journal of Engineering Physics and Thermophysics, Vol. 77, No. 3, 2004

INVESTIGATION OF THE MECHANISM OF RADIATION PROPAGATION AT SIDE ILLUMINATION OF A LIGHT GUIDE

G. F. Gornostaev, G. A. Frolov, and M. V. Trikula

UDC 536.3:681.586.5

A design of a fiber-optic distributed-type detector of radiation sources arbitrarily located in the technological control zone is proposed. We have elaborated a method for recording scattered and directed radiation flows supplied to the side surface of the optical fiber based on measurement of the luminous flux diffusely scattered by the technological microdefects of the optical fiber. It has been established that the scattered flux is concentrated mainly in the optical fiber cladding. The detector sensitivity to the radiation from a gas flame, a laser diode, and background sources has been investigated.

At present, more than a hundred types of fiber-optic detectors of physical quantities have been created. Practically all of them operate at end illumination of the optical fiber. In those cases where the location of the spatially distributed radiation sources is known exactly or their number is rather large, as well as where it is necessary to locate a radiation source, a large number of detectors with end illumination should be set up. To solve the above problems, it is interesting to consider a detector using the mechanism of radiation propagation at side illumination of the optical fiber.

To control the sparking at electric generator brushes, the appearance of an electric arc at contacts in the power cabinet, hydrogen inflammation in leakage from the turbogenerator casing, the radiant flux density distribution in a solar furnace, etc., a radiant flux detector recording distributed radiation sources is needed. Consider the possibility of developing a detector that allows one to record external radiation supplied to the side surface of the optical fiber using the radiation scattering by its internal technological microdefects (charge particles, air bubbles, etc.).

In light scattering, by the term "particles" is usually meant a small object consisting of many atoms. When objects are small compared to the light wavelength, the electrons in their atoms move almost simultaneously and equally in the light field. In this case, the scattering by particles of different sizes differs only in the amplitude, which depends on the number of electrons participating in the interaction [1]. The value of such (Rayleigh) scattering is $\sim\lambda^{-4}$, and its intensity weakly depends on the optical fiber temperature [2]. Ions of some impurities can also have a considerable effect on the light scattering [3].

When particle sizes form an appreciable part of the light wavelength or exceed it, the relative phase shifts in space and time between induced currents on the particle surface and inside it can cause complicated interactions between the incident and scattered light. Rigorous calculation of such scattering patterns even for relatively simple forms and parts of the structure is very complicated [4]. In the IR range, losses due to the scattering by particles amount to $\lambda^{-0.7}$ [5], i.e., they weakly depend on the source wavelengths.

Figure 1a shows a photograph of a glass optical fiber 14 mm in diameter illuminated by a flash bulb. Microdefects of size $\sim 10^{-3}$ mm (light dots) are the incident radiation scattering centers. Multiple reflections on these particles and their own luminescence create homogeneous radiation. It is distinct along the length of the optical fiber, and the greatest brightness is observed in the microdefects.

Figure 1b shows the scheme of visual observation of the end brightness at illumination of the side surface of the optical fiber. An optical fiber consisting of a pair of BF25–K17 glasses of diameter 1 mm and length 260 mm was illuminated from the side by a gas flame. The flame length is ~50 mm, the flame diameter is ~6 mm, and the dis-

I. N. Frantsevich Institute for Problems of Material Science, National Academy of Sciences of Ukraine, 3 Krzhizhanovskii Str., Kiev, 03142, Ukraine; email: frolov@alfacom.net. Translated from Inzhenerno- Fizicheskii Zhurnal, Vol. 77, No. 3, pp. 64–68, May–June, 2004. Original article submitted September 18, 2003.

1062-0125/04/7703-0543

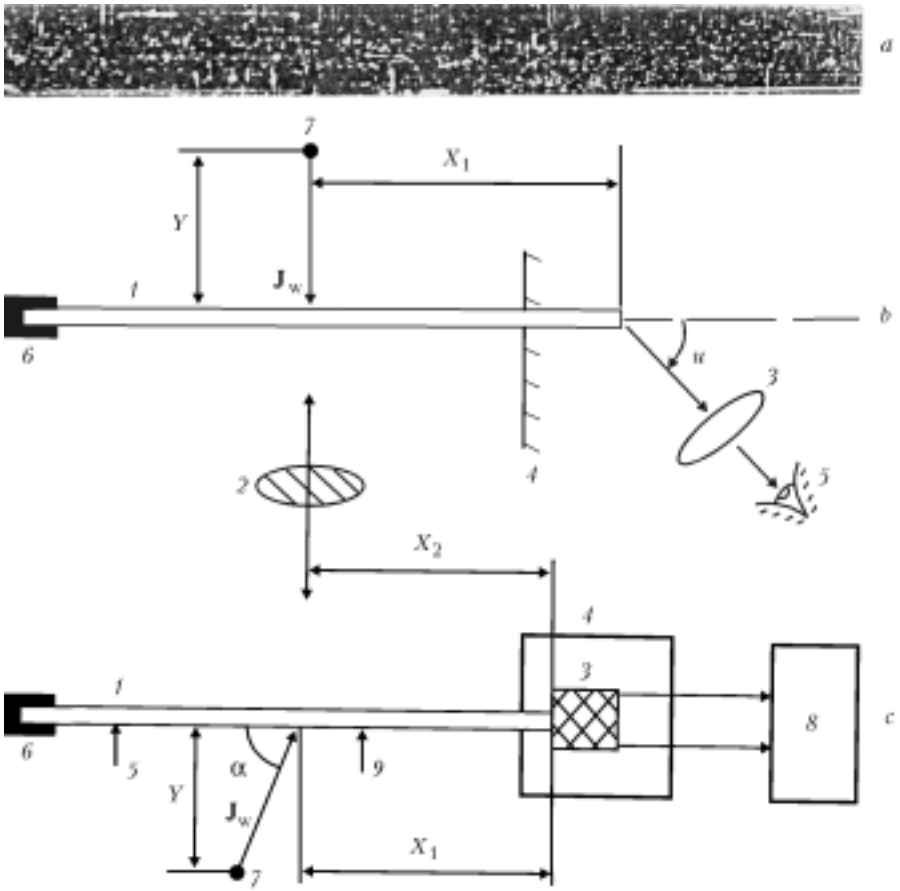

Fig. 1. Scheme of experimental investigations: a) optical fiber illuminated by a flash (light dots — microdefects); b) observation of the end brightness [1) optical fiber; 2) flame cross section; 3) lens; 4) screen; 5) eye; 6) cap; 7) laser diode]; c) measuring scheme [1, 2, 6, and 7) same as in Fig. 1b; 3) detector; 4) bush; 5) lamp; 7) multimeter; 9) daylight].

tance of the flame axis to the side surface of the optical fiber is ~100 mm. The distance from the flame axis to the plane in which the optical fiber end is located is ~100 mm, and background illumination is absent. As the second radiation source, a laser diode of power 10^{-3} W with a red light wavelength λ = 0.63–0.68 μm [6] was used. The beam diameter is ~4 mm, and the distance of the diode from the optical fiber surface is 150 mm.

The scheme for investigating the metrological possibilities of two types of optical fibers is given in Fig. 1c. The detector included an FP1-3 photoresistor (λ_m = 2.1 μm), a bush, an optical fiber, and a black cap. On the side, at a distance of 50 mm from the optical fiber surface a gas flame source was located, at a distance Y = 40 mm a laser diode was set up, and at a distance of 1.5 m an electric lamp of power 100 W was placed. A photodetector was connected to an Shch4313.1 multimeter. The distance X_2 = 100 mm. The first type is an optical fiber in a cladding (BF25-K17), the optical fiber length is 260 mm, the outer diameter is 1.0 mm, and the numerical aperture A_0 = 0.54. The second type is a rod with no cladding of diameter 3 mm made of optical glass. The black cap excludes photodetector illumination through the optical fiber end. The dark photoresistance was R_d = 140 kΩ.

At relatively large particle sizes compared to the wavelength the approach based on refraction and reflection (which are considered in the approximation of geometric optics) often appears to be effective in explaining various aspects of the light scattering by particles. In a limited range of angles, the Fresnel approximation of the scalar diffraction theory is applicable.

The scattering of light by the optical fiber material is proportional to its length and is one of the components of the total loss of light in the optical fiber [1]:

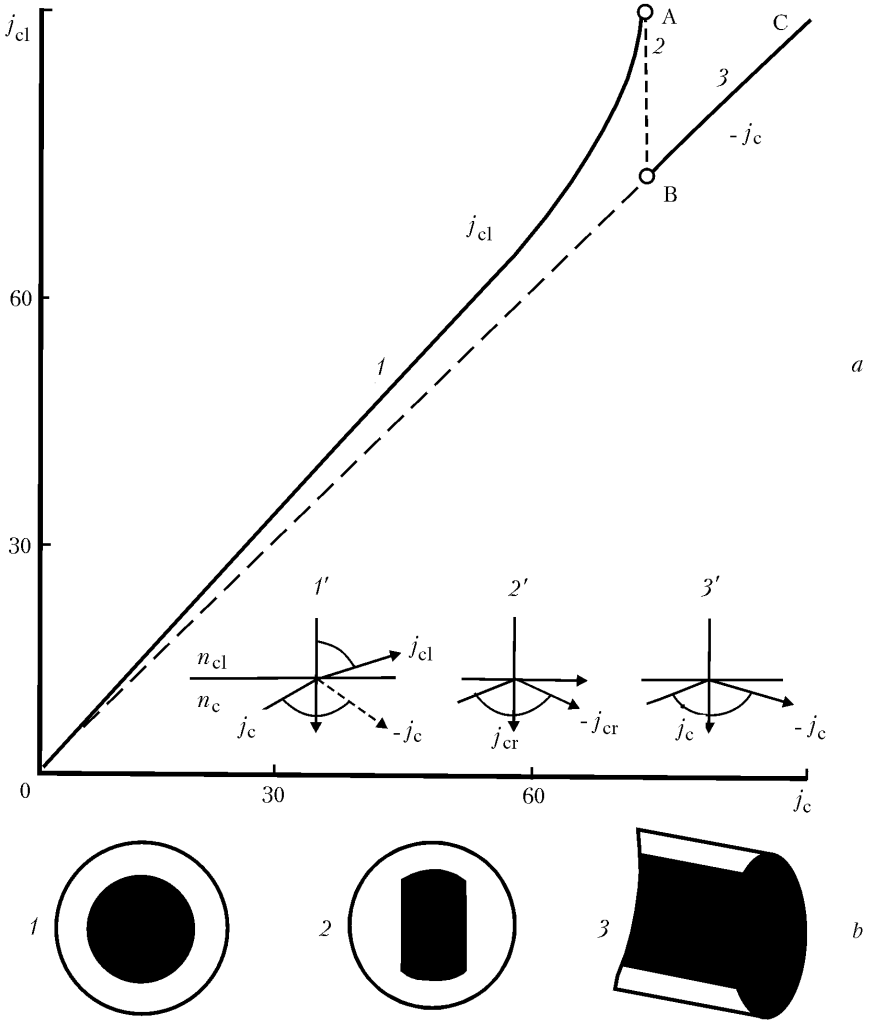

Fig. 2. Propagation of rays in the optical fiber: a) dependence of the angle of refraction of the ray in the cladding on the angle of incidence on the core–cladding boundary [1] [1) refraction of the ray; 2) boundary ray propagating along the optical fiber; 3) total internal reflection; b) results of the observations of the end brightness [1) $u = 0^o$; 2) $u \le 50^o$; 3) $u \ge 50^o$].

$$D_\lambda = D_{abs} + D_{ref} + D_F + D_e + D_s .$$

The expression for estimating complex radiation is of the form

$$D = -\lg \tau , \quad \tau = \int_0^\infty \tau_\lambda f d\lambda \Big/ \int_0^\infty f d\lambda .$$

The component that is due to light scattering by the optical fiber material weakly depends on the spectral composition of the radiation [7]. Here the governing factor is the integral density of the incident flux.

Consider the phenomena in the vicinity of the critical angle of the total internal reflection, which is equal to

$$j_{cr} = \arcsin (n_{cl}/n_c) .$$

Figure 2a shows the dependence of the refractive index of the ray in the cladding on the angle of incidence of the ray on the core (BF25 glass)–cladding (K17 glass) interface for the incident radiation wavelength $\lambda = 0.589$ μm

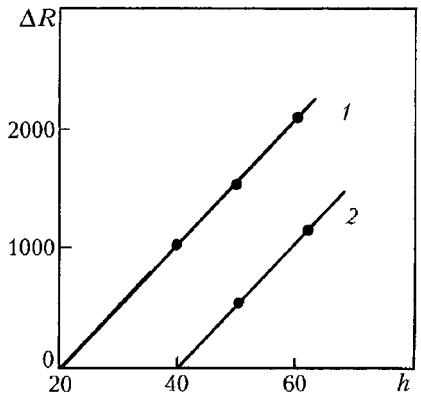

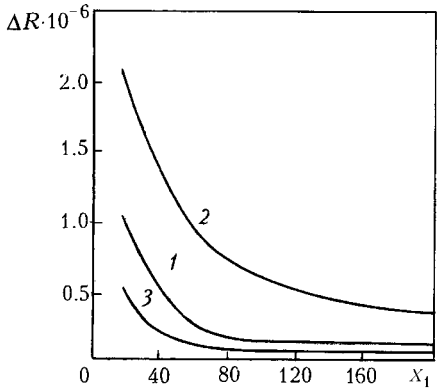

Fig. 3. Dependence of the change in the optical fiber photoresistance on the gas flame length h: 1) optical fiber of diameter 1 mm with a cladding; 2) optical fiber of diameter 3 mm without cladding.

Fig. 4. Dependence of the change in the detector photoresistance (SF3-1 detector, optical fiber of diameter 1 mm) on the linear and angular coordinate on the laser diode beam (Y = 40 mm): 1) α = 90; 2) 45; 3) 135°.

at an optical fiber length of 100 mm and a diameter of 20 μm [1]. At $j_c < j_{cr}$ (scheme 1′) a refracted (curve 0A) and Fresnel-reflected (curve 0B) ray exists. At $j_c = j_{cr}$ the angle of refraction reaches 90°. To this case correspond points A and B of the graph and scheme 2′. Points A and B correspond to the boundary case of the total internal reflection where there exist a reflected ray and a boundary ray propagating parallel to the optical fiber axis along the core–cladding boundary. At $j_c > j_{cr}$ (scheme 3′) only a totally internally reflected ray exist (straight line BC).

To determine which of the three considered schemes of radiation propagation dominates at side illumination of the optical fiber, we performed experiments on visual observation of the brightness of the output end through a lens (×5) at various angles with the optical fiber axis.

Figure 2b schematically represents the results of the visual observation (see Fig. 1b). At u = 0° against the background of the dark core the cladding ring shines brightly (1). As u is increased to about 50° (2), one can easily see two bright lines on the upper and lower elements of the optical fiber (along which the rays propagate), and the cladding end and two core sectors are bright. As the angle u is increased further, only the lines on the upper and lower elements of the optical fiber (boundary rays) remain bright (3). Thus, at side illumination of the optical fiber the major portion of the radiation propagates through the cladding and the peripheral part of the cross section due to the extra-aperture meridional rays and skew rays. Consequently, at side illumination the optical fiber operates according to scheme 1′ (Fig. 2a) much in the same manner as at end illumination in the case where $j_c < j_{cr}$. Since with decreasing illuminated area of the photosensitive layer of the photoresistor its sensitivity increases, it is expedient to set a focusing quarter-wave GRIN between the optical fiber end and the radiation detector.

The greater the ratio of the core diameter to the cladding diameter and the smaller the optical fiber aperture, the higher should, obviously, be the radiant power density passing through the cladding. Since the character of the output end brightness distribution is identical to the distribution at both diffuse heat radiation of the flame and directional monochromatic radiation of the laser diode, it may be concluded that the enormous number of microdefects create a statistical average light field, whose distribution over the optical fiber cross section weakly depends on the kind of radiator.

Meridional rays having a value of the angle $j_c > j_{cr}$ experience total internal reflection and propagate along the optical fiber core. However, their share is small, since the angular aperture of the BF25-K17 pair is only 30°. As a result, at end visual observation the optical fiber core looks dark and the cladding — light.

The presence of the edge effect (luminescence of the core sectors) is confirmation that the microdefects are diffuse radiators. Exactly the peripheral part of the optical fiber cross section exhibits the greatest ability to transmit ray bundles incident at large angles with the optical fiber axis, including diffuse radiation.

The results of the visual observation of the optical fiber end 3 mm in diameter without cladding at side illumination by a laser diode ray point to the fact that no radical changes in the law of radiation distribution over the

optical fiber cross section occur. On the surface of the optical fiber end only a thin ring of nonuniform width is luminescent. An edge effect analogous to that shown in Fig. 2b, position (2) is seen. In investigations with the use of two types of optical fibers (see Fig. 1c), the detectors were first illuminated by daylight, and then a lamp was switched on. The change in the photoresistance ΔR for the optical fiber of diameter 1 mm was 2000 Ω and for the optical fiber of diameter 3 mm — 1000 Ω. In the absence of daylight and electric light, a gas flame was initiated and the change in the photoresistance ΔR was registered at various lengths of the flame. For a flame diameter of ~6 mm, the experimental results obtained (Fig. 3) point to the fact that optical fibers of diameter 3 mm without cladding are of little use in radiation flow detectors with side illumination, and optical fibers of diameter 1 mm with cladding permit reliable measurements of the light signal of the flame.

The change in the photoresistance at illumination of an optical fiber 1 mm in diameter by a gas flame of length 40 mm (ΔR = 1000 Ω) is approximately equivalent to daylight or the addition to it of electric light. The change in the photoresistance at illumination of an optical fiber 1 mm in diameter by a flame of length 60 mm (ΔR = 2000 Ω) is approximately equivalent to the simultaneous action of daylight and electric light. Thus, to identify the radiation from a small-length gas flame, it is necessary to use a measurement algorithm invariant under the background radiation.

In using an SF3-1 photoresistor (λ_m = 0.78 μm) sensitive in the visible and near-IR regions of the spectrum, dependences of the change in the photoresistance of the detector on the linear and angular coordinates of the laser beam have been obtained (Fig. 4). The measuring scheme is given in Fig. 1c. A change in the distance from the laser diode to the side surface of the optical fiber in the 40–1000-mm range does not change the character of the curves [8]. Their shape is explained by the exponential dependence of the glass absorption intensity on the path length of the ray in the optical fiber. At $\alpha < 90^o$ the radiation flow onto the photodetector increases compared to the flow at $\alpha = 90^o$ because of the losses due to the reflection from the air–optical fiber cladding boundary. This is due to the lengthening of the scattering path of the transverse rays in the optical fiber as well as the growth of the portion of the incident flux propagating along the optical fiber. The latter factor is a consequence of the increase in the transmission coefficient of the optical fiber with increasing skewness of the rays at the core–cladding boundary.

At an angle $\alpha > 90^o$ (the flux is directed towards the capped end), only rays scattered by the microdefects of the glass strike the photodetector. This flux is weaker than the flux at $\alpha = 90^o$.

At the present time, algorithms for determining the value of the radiant power and coordinates of the radiator by means of the proposed detector are under development.

CONCLUSIONS

1. With the use of the diffuse scattering of light by random technological microdefects of the optical fiber that are relatively uniformly distributed along its length (Fig. 1a), diffuse and directive radiators located along a controlled path can be registered. In so doing, a panoramic view within $0–360^o$ with the optical fiber axis is provided.

2. Without an amplifier the sensitivity of a distributed-type optical-fiber detector in the IR region (λ_m = 2.1 μm) as well as in the visible region (λ_m = 0.78 μm) of the spectrum permits recording, respectively, the radiation from a gas flame of diameter 6 × 60 mm and a laser diode of power 10^{-3} W. The detector is able to yield information about the linear and angular coordinate of the laser beam. The employment of an amplifier will make it possible to increase the detector sensitivity by a few orders of magnitude.

3. The brightness distribution over the optical fiber cross section points to a diffuse scattering of radiation by microdefects, which together with the small value of the aperture angle (30^o) leads to the scattered radiation concentration in the optical fiber cladding. This result agrees with the scheme of radiation propagation at end illumination where $j_c < j_{cr}$.

NOTATION

A_0, numerical aperture of the optical fiber; D, dimensionless optical density of the optical fiber for complex radiation; D_e, dimensionless optical density of the optical fiber corresponding to the losses due to the influence of the edge effect; D_0, dimensionless optical density of the optical fiber corresponding to the internal reflection losses; D_{abs},

dimensionless optical density of the optical fiber corresponding to the losses due to light absorption by the optical fiber material; D_s, dimensionless optical density of the optical fiber corresponding to the scattering losses; D_F, dimensionless optical density of the optical fiber corresponding to the losses due to the Fresnel reflection from the ends; D_λ, dimensionless optical density of the optical fiber for monochromatic radiation; f, spectral density of the radiant flux, W/(m^2·μm); h, flame length, mm; $\mathbf{J}_w$, supplied radiant flux, W; j_{cl}, angle of refraction of the ray in the cladding, deg; j_c, angle of incidence of the ray at the core–cladding boundary; $-j_c$, angle of reflection of the ray from the core–cladding boundary, deg; j_{cr}, critical angle of incidence at which total internal reflection of the ray occurs, deg; $-j_{cr}$, angle of total internal reflection of the ray, deg; n_c, refractive index of the optical fiber core; n_{cl}, refractive index of the cladding; R, photoresistance, Ω; R_d, dark photoresistance, Ω; u, observation angle, deg; X_1, distance from the point of intersection of the optical fiber axis with the laser beam axis to the optical fiber end, mm; X_2, distance from the flame axis to the plane in which the optical fiber end is situated, mm; Y, distance of the radiator from the side surface of the optical fiber, mm; α, angle between the incident beam axis and the optical fiber axis, deg; ΔR, change in photoresistance, Ω; λ, radiation wavelength, μm; λ_m, wavelength of maximum photosensitivity of the photodetector, μm; τ, coefficient of complex radiation transmission by the optical fiber; τ_λ, spectral transmission coefficient of the optical fiber. Subscripts: c, core; e, edge effect; r, reflected; cl, cladding; abs, absorbed; cr, critical; s, scattered; d, dark; F, Fresnel reflection; m, maximum; w, side surface; λ, monochromatic; 0, optical fiber; 1, laser diode; 2, flame.

REFERENCES

1. G. F. Muchnik and I. B. Rubashov, *Methods of the Heat–Transfer Theory: Thermal Radiation* [in Russian], Vysshaya Shkola, Moscow (1974).
2. T. Okosi, K. Okamoto, M. Otsu, et al., *Fiber-Optic Sensors* [Russian translation], Énergoatomizdat, Leningrad (1990).
3. B. A. Krasyuk, O. G. Semenov, A. G. Sheremet'ev, and V. A. Shesterikov, *Fiber-Optic Sensors* [in Russian], Mashinostroenie, Moscow (1990).
4. H. Stark (Ed.), *Applications of Optical Fourier Transforms* [Russian translation], Radio i Svyaz', Moscow (1988).
5. G. G. Ishanin, É. D. Pankov, A. L. Andreev, and G. V. Pol'shchikov, *Radiation Sources and Detectors* [in Russian], Politekhnika, St. Petersburg (1991).
6. G. F. Gornostaev, Flame sensor for the system of hydrogen release from the turbo-generator, in: *Ext. Abstracts of Papers presented at Int. Conf. "Hydrogen Material Science and Chemistry of Metal Hybrids"* [in Russian], Kiev (2001), pp. 796–797.
7. V. B. Veinberg and D. K. Sattarov, *Optics of Light Guides* [in Russian], Mashinostroenie, Leningrad (1977).
8. G. F. Gornostaev, V. Ya. Berezhetskaya, and A. V. Shevchenko, Development of sensors for diagnostics of power engineering equipment, in: *Proc. Int. Conf. "Estimation and Substantiation of Prolongation of Service-Life of Members"* [in Russian], Vol. 2, Kiev (2000), pp. 587–592.